10.1149/1.3205005 © The Electrochemical Society

Oxidation and Creep Behavior of Porous E-Brite for Solid-Oxide Fuel Cell Interconnects

J. A. Scott and D. C. Dunand

Department of Materials Science & Engineering, Northwestern University
Evanston, Illinois 60208, USA

The effects of isothermal oxidation on the creep response and porosity of E-Brite foams at 800ºC were investigated. Samples of 43.2% and 51.4% porosity were first oxidized in static laboratory air up to 200 hours to determine oxidation kinetics. Select samples were removed after 10 and 100 hours of oxidation and then creep tested to characterize the impact of scale growth on mechanical response and changes in porosity. Significant creep strengthening was observed even when minimal oxide growth occurred. Although oxide growth led to reduced pore size and choked fenestrations, the reduction in open porosity after 200 hours of exposure remained less than 10%.

Introduction

Recent reductions in solid oxide fuel cell (SOFC) operating temperatures permit the use of metallic interconnects in place of ceramics but their application remains a challenge. Potential alloys are limited due to the harsh environmental conditions imposed by simultaneous exposure to an oxidizing and reducing atmosphere at elevated temperatures as high as 800ºC (1). Given the requirements of service, chromia-forming ferritic steels remain one of the most popular candidate families of alloys to examine for interconnect components due to their electrically conducting oxide, coefficient of thermal expansion match with the stack, and low cost. Several studies have investigated the oxidation behavior, thermal expansion, and electrical properties of dense ferritic steels in traditional SOFC operating conditions (1-3). Little work, however, has examined these properties in light of a new class of porous interconnects being developed for planar SOFCs.

Porous interconnects are proposed to help reduce the weight and cost of the stack while simultaneously serving as flow channels for the fuel and oxidant (4-11). Most porous interconnect substrates are prepared using powder metallurgy techniques with porosities in range of 30% – 50% (9-14). The increased surface area of these porous structures, however, can lead to rapid oxidation (10). Oxidation can significantly affect the performance of the interconnect and, to date, most work involving porous interconnects has focused on the resulting change in area specific resistance (ASR) (7, 10). However, the thickness of oxide scale influences mechanical properties and leads to choking of pore fenestrations or connections, which can impede fluid flow. Accordingly, ferritic steel samples with porosities ca. 40% and 50% were prepared and tested to determine the effect of oxidation on mechanical response and the reduction in fenestration size at various growth intervals.

Experimental Procedures

E-Brite (Fe-26Cr-1Mo, wt.%) is a commercial ferritic steel alloy and was chosen as the subject of this study due to its coefficient of thermal expansion match with ceramic SOFC components, oxidation resistance, and low material cost (1). Samples were prepared by first combining elemental powders of Fe (APS 6-10 μm), Cr (APS < 10 μm), and Mo (APS 3-7 μm) acquired from Alfa Aesar (Ward Hill, MA) in the appropriate weight fraction. The resulting mixture was tumbled end over end at 30 RPM for one hour. NaCl was then crushed and sieved to a size of 53-106 μm. Subsequently, NaCl powder was added to the E-Brite powder mixture in the appropriate volume fraction and again mixed end over end at 30 RPM for one additional hour. The mixture was then uniaxially cold pressed at 350 MPa and vacuum sintered at 1250°C for 4 hours, whereupon the NaCl place holder evaporated and the metallic powders interdiffused and densified.

Foams with total porosities within 3% of the target value were achieved, each with a closed porosity of less than 2%. Closed porosity of specimens prior to oxidation was determined by helium pycnometry based on a known bulk density of 7.69 g/cm^3 for E-Brite. To obtain open porosity, Archimedes density measurements were performed after coating porous samples with a thin layer of vacuum grease to prevent infiltration of water into the open porosity. When reporting porosity, the total (open plus closed) porosity is used unless otherwise specified.

Prior to oxidation, cylindrical compression samples were machined for mechanical testing. Specimens were then placed on an alumina boat and isothermally oxidized in static laboratory air (uncontrolled humidity) in a muffle furnace at 800ºC for up to 250 hours. Samples were periodically returned to ambient temperature to allow measurement of weight gain from oxidation. The weight increase was normalized by surface area, which was determined as follows. Foams with 40% and 50% porosity were simultaneously oxidized for ~5 hours with an E-Brite plate with an easily determinable surface area. Weight gain of each sample was measured individually and foam surface area was estimated under the assumption that it was proportional to the increase in weight. This allowed for calculation of the parabolic rate constants from the measured oxidation curves.

Cylindrical samples for mechanical testing were prepared by wire electro-discharge machining the sintered compacts to dimensions of 6 mm (D) × 12 mm (H). A total of three specimens were machined from each compact to determine creep response of samples that were non-oxidized, preoxidized 10 hours, and preoxidized 100 hours. Creep was measured in compression using an ATS Series 3210 compressive creep frame with a lever arm arrangement. Displacement was measured by a LVDT that directly monitored deflection of the alumina pushrod to an accuracy of 6 μm. A testing temperature of 800°C was chosen to simulate typical SOFC operating conditions and was achieved by means of a three-zone, resistively-heated furnace with a temperature stability of ±2°C. A retort setup was assembled inside the furnace using a quartz tube to enable flowing argon and ensure negligible oxidation throughout the course of the test. Constant-load creep tests were performed until accumulated strains were a maximum of 0.1 to ensure consistency of structure among samples tested. Up to four increasing loads were applied

on a single sample. Corresponding secondary creep rates were determined by the slopes of strain-time plots acquired for each stress.

Specimens were cross-sectioned, mounted in an epoxy resin, and polished using standard metallographic procedures. Polishing was finished with a 0.05 μm Al_2O_3 slurry. Optical microscopy and SEM were used to examine the microstructures of foams and oxide scale growth.

Results

Oxidation Behavior

Figure 1 displays the kinetics of mass gain at 800ºC in static laboratory air up to 200 hours for four E-Brite foams: two at 43.2% porosity and two at 51.4% porosity. When normalized by mass as in Figure 1(a), the 51.4 % porous foams exhibit higher mass gain than the 43.2% porous foams as expected due to the difference in surface area. However, if normalized by surface area as in Figure 1(b), no difference is observed within experimental error, indicating the mechanism of oxidation for the two foams are the same in the static air environment.

Based on Wagner's oxidation theory, when scale growth is dominated by diffusion, it can be predicted by the parabolic dependence:

$$(\Delta m)^2 = K_p \times t, \qquad [1]$$

where Δm is mass gain per unit area, K_p is a parabolic rate constant, and t is time. It has been shown in previous work that this may not be a suitable prediction for long-term behavior due to the variance of K_p over time (15). Such deviation from linearity is evident in Figure 2, which plots Δm as a function of t. Thus, a more appropriate method of comparison is to determine the instantaneous value of K_p, which was accomplished by computing the slope of every pair of neighboring data collected. The resulting range of K_p values for the samples tested are seen in Table I.

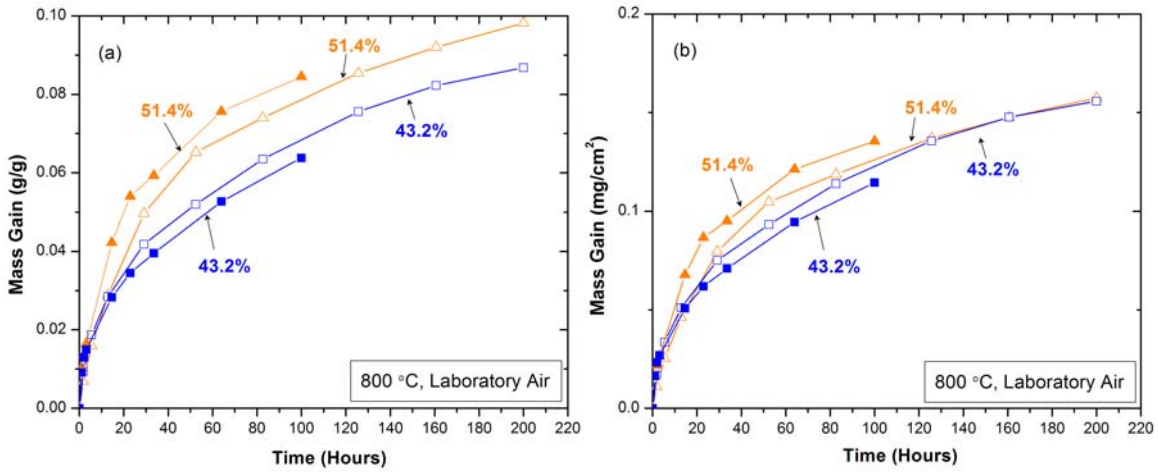

Figure 1. Isothermal oxidation kinetics for 43.2% and 51.4% porous E-Brite foams at 800ºC in static laboratory air, with mass gain normalized by (a) sample weight and (b) sample surface area.

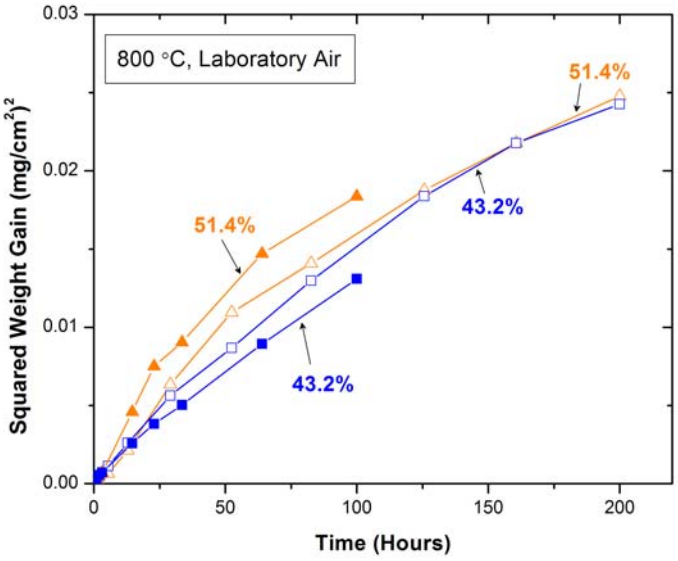

Figure 2. Isothermal oxidation kinetics for E-Brite foams at 800ºC in static laboratory air with the square of weight gain normalized by sample surface area.

TABLE I. Comparison of mean parabolic constant values for 43.2 % and 51.4 % porous E-Brite and previously reported literature values.

Material	Mean K_p ($\times 10^{-13}$ g^2 cm^{-4} s^{-1})
43.2 % Porous E-Brite	0.29 - 0.94
51.4 % Porous E-Brite	0.42 - 0.55
Dense E-Brite (1)	0.353
Dense E-Brite (16)	0.88

Figure 3 reveals the pyramid-like morphology of the Cr_2O_3 scale consistent with previous work on E-Brite oxidation in air (1, 17). As the scale grows it begins to decrease pore size and choke fenestrations, thus reducing open porosity as reported in Table II. The decrease in open porosity is visible in the series of optical micrographs shown in Figure 4 for 0, 10, 100, and 200 hours of oxidation in static laboratory air at 800ºC.

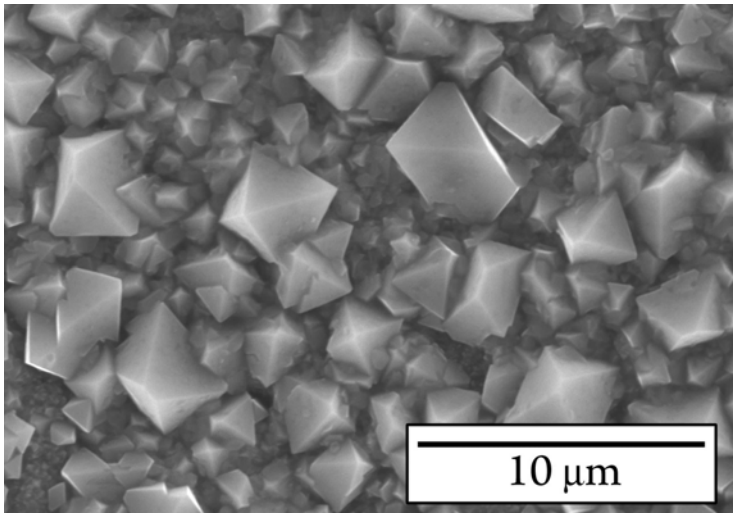

Figure 3. SEM of Cr_2O_3 scale morphology on E-Brite surface after 100 hours of exposure at 800ºC in static laboratory air.

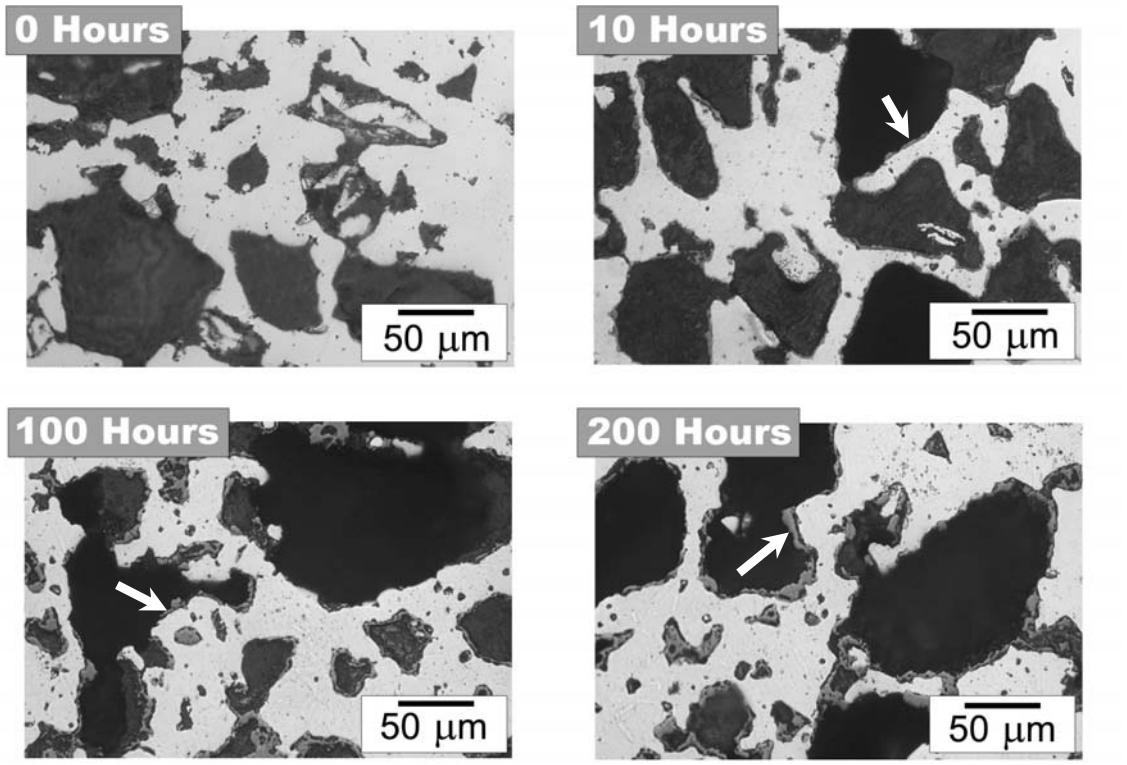

Figure 4. Optical micrographs of polished cross sections for 51.4% porous E-Brite foam after 0, 10, 100, and 200 hours of exposure at 800°C in laboratory air. Oxide (dark gray) is visible at the edge of the E-Brite matrix (white) after just 10 hours of exposure. Some areas of larger scale thickness are highlighted with arrows.

Table II. Porosity values for samples containing 43.2 % and 51.4 % total porosity at various lengths of exposure to static laboratory air at 800 ºC.

Exposure Time (Hours)	Sample Open Porosity (%)	Sample Open Porosity (%)
0	50.6 (51.4 Total)	42.0 (43.2 Total)
10	46.0	38.4
100	44.0	36.0
200	40.9	32.5

Creep Properties

A typical compressive strain-time plot is shown in Figure 5 for a 43.2 % porous E-Brite foam preoxidized for 10 hours prior to creep testing. All creep curves exhibited similar behavior consisting of an initial stage of primary creep followed by a secondary stage where the average strain rate was constant. Samples were removed prior to tertiary stage creep (i.e., before densification).

All creep data obeyed typical power-law behavior:

$$\dot{\varepsilon} = A\sigma^{n} \exp\left(\frac{-Q}{RT}\right) \qquad [2]$$

where A is the Dorn constant, n the stress exponent, Q the activation energy, R the gas constant, and T is temperature. Figure 6 is a double logarithmic plot of minimum strain rate, $\dot{\varepsilon}$, as a function of applied stress, σ, at a typical SOFC operating temperature of 800 °C for 43.2 % and 51.4 % porous E-Brite preoxidized for 0, 10, and 100 hours. Best-

fit apparent stress exponents are all in the range of 2.8 – 4.6, expected with dislocation-dominated, power-law creep.

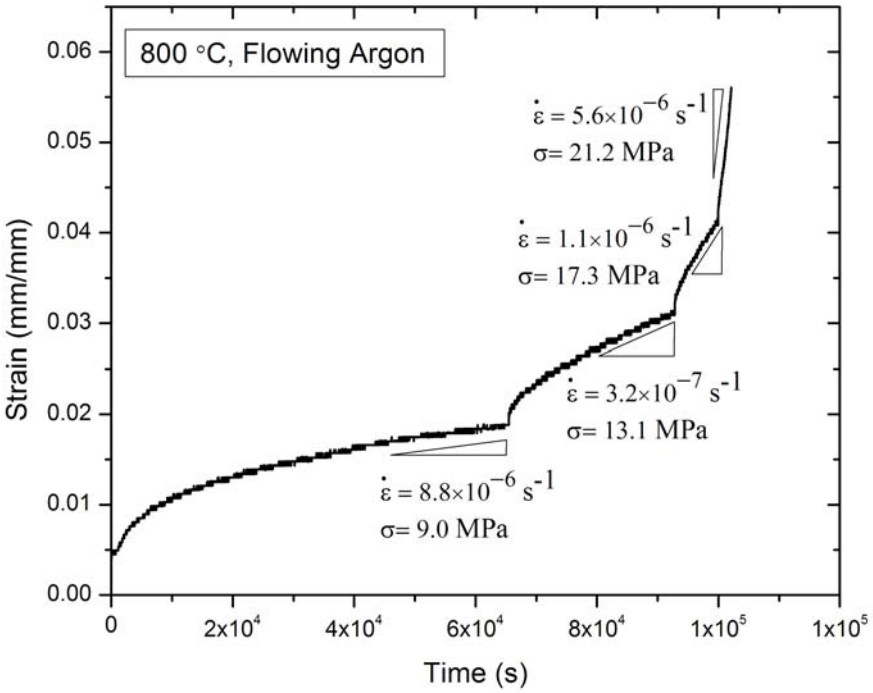

Figure 5. Typical compressive strain-time plot of a 43.2% porous E-Brite foam, preoxidized for 10 hours. Two regions of behavior are visible: primary creep followed by secondary, steady-state creep.

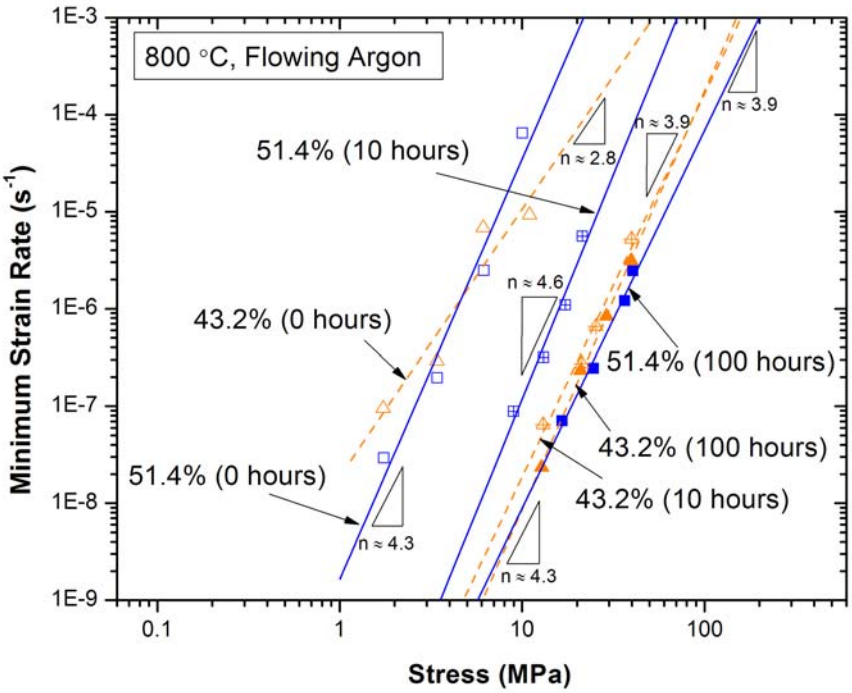

Figure 6. Secondary steady-state compressive creep rate plotted as a function of applied stress for porous E-Brite tested at 800°C under flowing Ar. Values in parentheses indicate hours of preoxidation prior to creep testing.

Discussion

The range of values for parabolic oxidation rates of porous E-Brite correlates well with previously reported values for the bulk material. Among chromia-forming ferritic steel alloys, this rate is low compared to potential interconnect alloy alternatives such as 430 or 446 (1). Cracking and spallation nonetheless remain an issue with chromia forming alloys, particularly during prolonged exposure and when subject to thermal cycling (18). Consequently, coatings containing reactive elements are recommended to control growth, improve adherence, and maintain consistent behavior over the lifetime of the fuel cell (16,19).

Though scale growth continues well beyond 200 hours of exposure, further decreases in porosity induced by pore choking diminish beyond this time, consistent with the mass gain trend in Figure 1. This is evidenced by Table II and implies that a larger initial porosity can be used to maintain a desired threshold for percolation of the foam. Due to the oxide morphology, seen in Figure 3, it is not expected that significant additional closed porosity is likely. The majority of reduced porosity appears to stem from the reduction in pore size. Given the composite nature of the material, it was not possible to analyze the reduction in closed porosity using pycnometry. Usable open porosity was nonetheless determined and indicates that after 200 hours of exposure, a ~10% change in absolute porosity occurs.

Significant creep strengthening is observed in the case of oxidized samples. With just 10 hours of oxidation, strain rats are ca. 100 times lower. This behavior is in accordance with the anticipated reduction in porosity and growth of the oxide skeleton that serves to strengthen the E-Brite foams.

It is important to note that the results of this study are most directly applicable to behavior on the anode side of the SOFC where the E-Brite is exposed to an oxidizing environment. A better understanding of the mechanical response of porous E-Brite and composite effects due to oxidation in a reducing environment is needed to fully characterize behavior in the SOFC stack. Previous work identifies anomalous behavior in dual-exposure conditions (1,17), which should also apply to porous materials, though additional work is needed to further examine this effect.

Conclusions

The oxidation kinetics at 800ºC of E-Brite foams with porosities of 43.2% and 51.4% are similar to those of the bulk material. Although the increased surface area of higher porosities leads to larger mass gains, the correspondence of parabolic rate constants with previously reported values indicates the difference in porosity does not affect oxide scale growth. Upon oxidation at 800ºC, however, mechanical properties of E-Brite foams are significantly influenced by the presence of oxide scale. After just 10 hours of exposure in static laboratory air, a difference in strain rate of nearly 100 times is observed. Though this creep strengthening effect diminishes with increasing exposure, its rapid occurrence alters the mechanical properties of the interconnect and should be acknowledged in the initial design of the stack. Preoxidation is one method that may help ensure more consistent performance of the fuel cell stack throughout its lifetime. Furthermore, if the oxide scale is dense enough and is able to resist spallation, the continuous Cr_2O_3 network may lead to changes in the coefficient of thermal expansion of the interconnect. This

could be addressed with a method such as preoxidation. As oxide scale grows in E-Brite foams, pore fenestrations are choked, resulting in reduced porosity. This can be problematic in the case where foams are intended for use as fluid flow channels. Results indicate that larger initial porosities can be used to ensure desired percolation in the interconnect after oxide growth.

Acknowledgments

The authors acknowledge Dr. R Bhat (GE Global Research Center) for useful discussions. This research was funded by NASA through a subcontract from GE (Award NNC06CB31C). JAS also thanks Bell Labs, the National Science Foundation, and the Nanoscale Science and Engineering Center at Northwestern University for graduate research fellowships.

References

1. Z. Yang, K. S. Weil, D. M. Paxton and J. W. Stevenson, *J. Electrochem. Soc.*, **150**, A1188 (2003).
2. J. W. Fergus, *Mater. Sci. Eng., A*, **397**, 271 (2005).
3. W. J. Quadakkers, J. Piron-Abellan, V. Shemet and L. Singheiser, *Mater. High Temp.*, **20**, 115 (2003).
4. M. Lang, T. Franco, G. Schiller, N. Wagner, *J. Appl. Electrochem.*, **32**, 871 (2002).
5. S. Takenoiri, N. Kadokawa and K. Koseki, *J. Therm. Spray Technol.*, **9**, 360 (2000).
6. N. Brandon, D. Corcoran, D. Cummins, A. Duckett, K. El-Khoury, D. Haigh, R. Leah, G. Lewis, N. Maynard, T. McColm, R. Trezona, A. Selcuk and M. Schmidt, *J. Mater. Eng. Perform.*, **13**, 253 (2004).
7. S. Molin, B. Kusz, M. Gazda and P. Jasinski, *J. Power Sources*, **181**, 31 (2008).
8. J. D. Carter, T. A. Cruse, J.-M. Bae, J. M. Ralph, J. M. Deborah, R. Kumar and M. Krumpelt, *Mater. Res. Soc. Symp. Proc.*, **756** (2003).
9. I. Villarreal, C. Jacobson, A. Leming, Y. Matus, S. Visco and L. De Jonghe, *Electrochem. Solid-State Lett.*, **6**, A178 (2003).
10. I. Antepara, I. Villarreal, L. M. Rodríguez-Martínez, N. Lecanda, U. Castro and A. Laresgoiti, *J. Power Sources*, **151**, 103 (2005).
11. R. Vaßen, D. Hathiramani, J. Mertens, V. A. C. Haanappel and I. C. Vinke, *Surf. Coat. Technol.*, **202**, 499 (2007).
12. Y. B. Matus, L. C. De Jonghe, C. P. Jacobson and S. J. Visco, *Solid State Ionics*, **176**, 443 (2005).
13. P. J. Panteix, V. Baco-Carles, P. Tailhades, M. Rieu, P. Lenormand, F. Ansart and M. L. Fontaine, *Solid State Sci.*, **11**, 444 (2009).
14. E. Arahuetes, A. Bautista, F. Velasco, M. E. Sotomayor, *Rev. Metal.*, **44**, 406 (2008).
15. Y. Liu, *J. Power Sources*, **179**, 286 (2008).
16. K. Huang, P. Y. Hou and J. B. Goodenough, *Mater. Res. Bull.*, **36**, 81 (2001).
17. Z. Yang, M. S. Walker, P. Singh, J. W. Stevenson and T. Norby, *J. Electrochem. Soc.*, **151**, B669 (2004).
18. W. N. Liu, X. Sun, E. Stephens, M. A. Khaleel, *J. Power Sources*, **189**, 1044 (2009).
19. Z. Yang, G.-G. Xia, X.-H. Li and J. W. Stevenson, *Int. J. Hydrogen Energy*, **32**, 3648 (2007).